Journal of Structural Geology, Vol. 6, No. 6, pp. 711 to 719, 1984
Printed in Great Britain

0191-8141/84 $03.00 + 0.00

The curved translation path of the Parpaillon Nappe (French Alps)

O. MERLE and J. P. BRUN*

Centre Armoricain d'Etude Structurale des Socles (CNRS) Université de Rennes, 35042 Rennes Cedex, France

(*Received* 11 *July* 1983; *accepted in revised form* 19 *January* 1984)

Abstract—The Parpaillon Nappe is one of the two Helminthoid Flysch nappes emplaced on the external Dauphinois zone of the Western Alps. A structural analysis of the nappe is presented. Two superposed deformations *D*1 and *D*2 are described, that are mainly characterized by large-scale recumbent folds whose axes are quasi-orthogonal: NE–SW for *D*1 and NW–SE for *D*2. Their vergence is northwestward for *D*1 and southwestward for *D*2. During the *D*2 deformation, the nappe was separated into two units, one of these being thrusted over the other. An analysis of incremental strain using quartz and calcite fibre growth indicates that *D*2 follows *D*1 without discontinuity. Therefore the superposition of *D*1 and *D*2 structures is interpreted as a progressive deformation instead of two distinct phases of deformation. The emplacement of the nappe is discussed under two aspects, the relations between displacement and strain and the role of gravity. It is concluded that the translation has been twofold, first towards the NW and then towards the SW, and that the displacement result essentially from gravity forces. Kinematic implications for the Alpine collision are suggested.

INTRODUCTION

THE PARPAILLON Nappe is one of the two large 'Helminthoid Flysch' nappes emplaced on the Dauphinois zone between the Pelvoux and Argentera crystalline massifs in the French Alps (Fig. 1). A geological map based on detailed stratigraphy and analysis of large-scale structures has been previously provided by Kerckhove (1969). More recently, an analysis of large- and small-scale structures has shown that two superposed deformation events are represented in the nappe (Merle & Brun 1981) and a sequential emplacement model has been proposed (Merle 1982a).

The purpose of this paper is (a) to examine the relationship between the superposed structures and progressive deformation as a consequence of a curved translation of the Parpaillon Nappe towards the NW during the Oligocene and towards the SW during the Miocene and (b) to discuss the role of gravity. We first describe the geometry of *D*1 and *D*2 structures at the scale of the nappe. Secondly, an analysis of quartz and calcite fibres in veins and pressure shadows is presented. Lastly, the discussion is devoted to the relations between strain and the nappe translation, and to the role of gravity.

GEOLOGICAL SETTING

Several nappes have been preserved in the depression between the Pelvoux and Argentera crystalline massifs (Fig. 1). In this area, a thick Mesozoic and Cenozoic sedimentary cover (about 7 km) is deposited over the basement. The last member of the pile constitutes the nummulitic formations deposited during the late-Eocene generalized transgression. This thick cover has undergone one and locally two deformations before the emplacement of the nappes. The allochthonous material may be separated into three principal nappes and two superposed structural units.

The lower structural unit is constituted by the sub-Briançonnais nappes and the Autapie Helminthoid Flysch nappe. The sub-Briançonnais nappes display a very complex arrangement of numerous slices (Kerckhove 1969, Maury & Ricou 1983). Their facies range from Upper Triassic to Upper Eocene. The Autapie nappe exhibits characteristic Helminthoid calcareous facies and shows much evidence for subaqueous

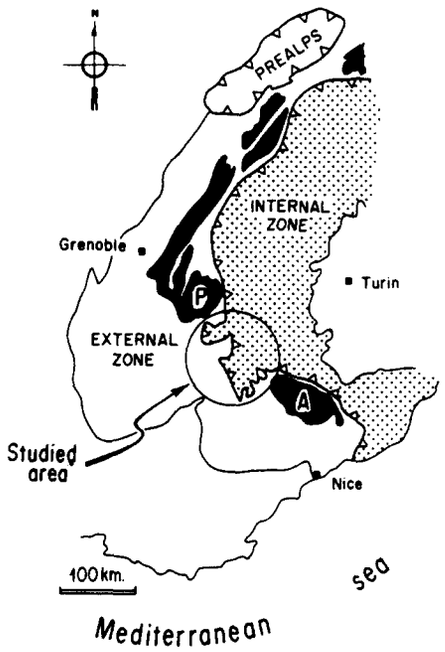

Fig. 1. Location of the studied area. Crystalline massifs shown in black: P, Pelvoux and A, Argentera.

*Present address: Département des Sciences Physiques de la Terre, Université de Paris VII, 2 place Jussieu, 75221 Paris Cedex 05, France.

emplacement (Kerckhove 1969). The sub-Briançonnais nappes and the Autapie nappe were folded together during the late Oligocene phase. Their emplacement in the Embrunais–Ubaye area is thought to take place during the early Oligocene.

The upper structural unit is the largest Helminthoid Flysch nappe called the Parpaillon Nappe. The stratigraphy of this Upper Cretaceous flysch is well-known (Latreille 1961, Kerckhove 1969) and constitutes a thin (50–100 m) dark shale layer at the base overlain by 1000–2000 m of typical Helminthoid limestones. In the Embrunais area, a detritic sandstone layer is transitional between these two facies. The Parpaillon Nappe lies on an erosional surface which cross-cuts the Oligocene structures of the Digne thrust sheet. Consequently, the final emplacement of the Parpaillon Nappe in Embrunais–Ubaye probably occurred during the early Miocene (Kerckhove 1969). The 'Helminthoid Flysch' sequences of the Autapie and Parpaillon nappes were deposited in the Ligurian Ocean at the end of Cretaceous time. Their Eocene tectonic history was unknown before this study.

METHOD OF STRUCTURAL ANALYSIS

Results presented here have been obtained from a simultaneous use of the following.

(1) Geological and structural mapping.

(2) Construction of a series of balanced cross sections (Hossack 1979).

(3) Estimation of horizontal shortening variations from balanced cross sections. Different methods have been used (Elliott 1977, Hossack 1979) and the results compared (Merle 1982b).

(4) Incremental strain variations from calcite and quartz fibres in pressure-shadows around rigid objects and in veins (Durney & Ramsay 1973).

(5) Estimation of the shape of finite strain ellipsoids from shape ratios of pressure shadows around rigid objects (Choukroune 1971). Unfortunately, it has not been possible to determine more precisely the geometrical parameters of finite strain ellipsoids.

(6) Determination of finite shear sense from small-scale structures (Choukroune & Lagarde 1977, Lagarde 1978, Berthé *et al.* 1979).

(7) Analysis of minor fold shapes (dip isogons and layer thickness–dip variations, Ramsay 1967).

Detailed results are given in Merle (1982b) whose main conclusions are summarized in the following sections. The kinematic analysis has been coupled with small-scale experiments concerning nappe emplacement (Brun & Merle 1982) whose detailed results will be published elsewhere.

SUPERPOSED STRUCTURES

Two superposed folding events $F1$ and $F2$ with orthogonal axial directions have been demonstrated in the Parpaillon Nappe (Merle & Brun 1981). Each event is characterized by a pressure-solution cleavage, a stretching lineation and recumbent folds. Their superposition may be observed in many places by $F1$–$F2$ fold interference patterns and deformation of $S1$ cleavage and $L1$ lineation by $F2$ folds. Geometrical features of these two deformations show remarkably regular orientations at the scale of the nappe (Fig. 2).

The D1 *deformation*

The early deformation event, $D1$, is characterized by isoclinal recumbent folds overturned towards the NW with a mean axial trend N50°E. Major and minor folds are relatively scarce and have been observed only at the base of the nappe. They are similar (class 2, Ramsay 1967), and the associated axial-plane cleavage appears at most places parallel to the stratification. The stretching lineations observed on the cleavage plane have a mean direction N140°E, orthogonal to the fold axes (Fig. 2a). Geometrical analysis of syntectonic quartz–calcite veins, deformed sedimentary structures and shapes of pressure shadows (Choukroune 1971) around detrital quartz grains (see next section) demonstrate that finite strain ellipsoids are of the flattening type ($0 < k < 1$, where $k = (X/Y - 1)/(Y/Z - 1)$ and $X \geq Y \geq Z$ are the principal axes of the strain ellipsoid. Discrete slip toward the NW along the stratification and the $S1$ cleavage are demonstrated by relative displacement of veins, step structures and quartz–calcite fibre growths on the activated discontinuities.

The D2 *deformation*

The $D2$ deformation is the most obvious in the landscape. It is characterized by large and numerous large-scale recumbent folds with a SW vergence, and a mean axial trend N140°E. All stratigraphic units and $S1$ cleavage are deformed by the $F2$ folds. An $S2$ cleavage, showing a fan disposition, is generally observed in the hinges but not always in the limbs where the $S1$ cleavage is often completely preserved. Because of the very heterogeneous deformation, where no $S1$ cleavage has been developed, the $S2$ cleavage is locally the only cleavage observed. The associated stretching lineation has a mean trend N50°E (Fig. 2b). The detail description of the $D2$ structures is best achieved by separating the nappe into two units (Merle 1982a, b).

(A) *Unit* 1. The first unit constitutes the eastern part of the nappe (Fig. 3a). It is, as a whole, a large syncline overturned towards the SW and bounded eastward by the thrusted Briançonnais series. The following facts must be accounted for.

(1) Unit 1 is folded with its substrata (Fig. 3b).

(2) The deformation intensity decreases as one goes from the Briançonnais thrust to the west (Fig. 3c).

(3) The deformation intensity is at a maximum just

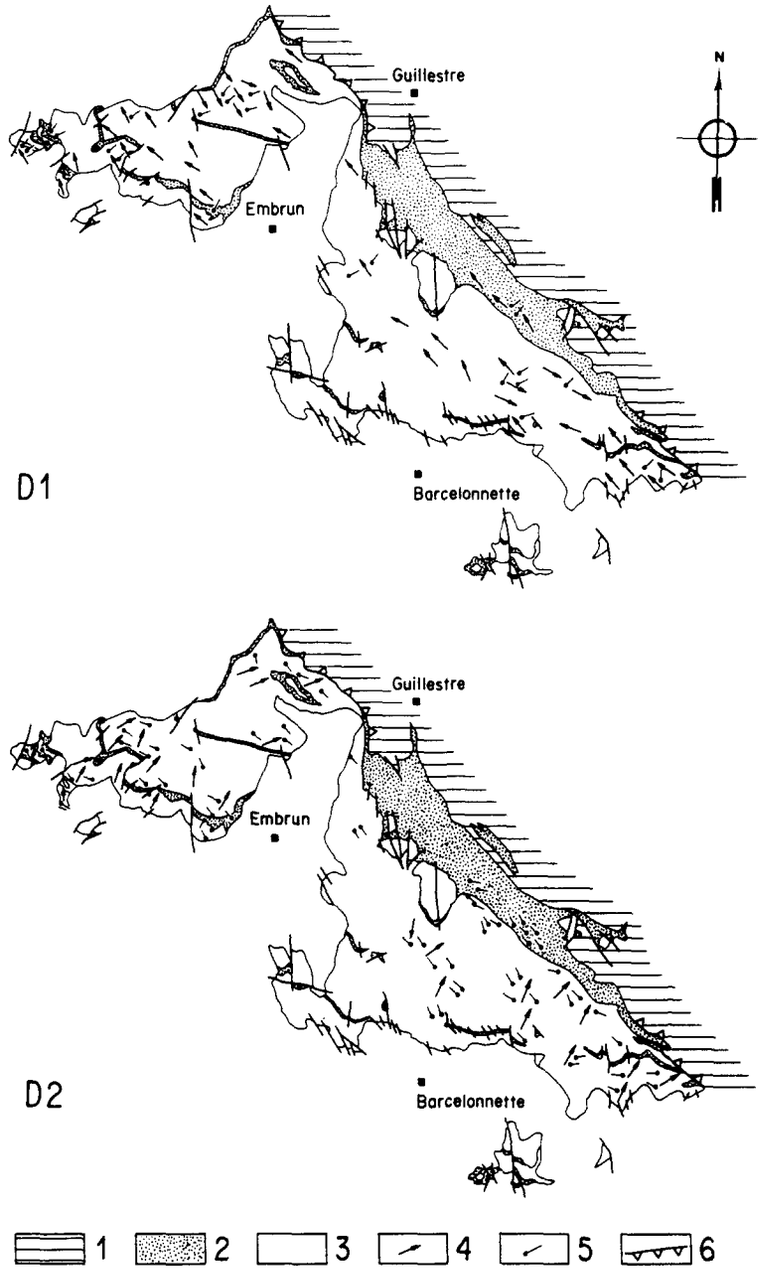

Fig. 2. Structural maps of the Parpaillon Nappe: upper map is *D*1 data and lower map *D*2. 1, Briançonnais Series; 2, basal layer (dark shales); 3, Calcareous flysch (Helminthoid Flysch s.s.); 4, stretching lineations; 5, fold axes and 6, Briançonnais thrust.

under the Briançonnais thrust where it is accompanied by a low-grade metamorphism (Tricart 1980).

The *D*2 deformation in unit 1 is clearly related to the Briançonnais thrusting and therefore can be dated as late-Oligocene. In the northern part, a slice separated from the rest of unit 1 by thrust faults is not affected by the *D*2 deformation and indicates a northward thrusting onto sedimentary cover of the Pelvoux Massif (Fig. 1) during the *D*1 deformation.

(B) *Unit* 2. Unit 2 extends to the west of unit 1 (Fig. 3a). The base of this unit is a Miocene erosional surface cross-cutting Oligocene structures (Kerckhove 1969). The *D*2 deformation in unit 2 therefore appears to be later than in unit 1. In this unit, the horizontal shortening increases towards the front (Fig. 3c), and major *F*2 folds are located in depressions of the Miocene erosion surface and at the front (Fig. 3b).

Unit 1–*Unit* 2 *relationships*

The contact between the two units has not been observed in the field. Nevertheless, because in the two units, (a) the sense of horizontal shortening variation is inverse, (b) the timing of *D*2 deformation is slightly different (Oligocene in unit 1 and Miocene in unit 2) and (c) horizontal klippes over unit 1 (Figs. 3a & b) are associated with an intense deformation of the top part of unit 1, as demonstrated by strongly developed cleavage and large-scale sheath folds, we deduced (Merle 1982a) that unit 2 has slid over unit 1 (Fig. 4).

The analysis of structures and fabrics (Merle 1982b) shows that *D*2 deformation corresponds to a dominant shearing more or less parallel to the layering. At the upper levels of the nappe, the resulting strain is of plane strain type ($k \simeq 1$). At the base, pressure shadows

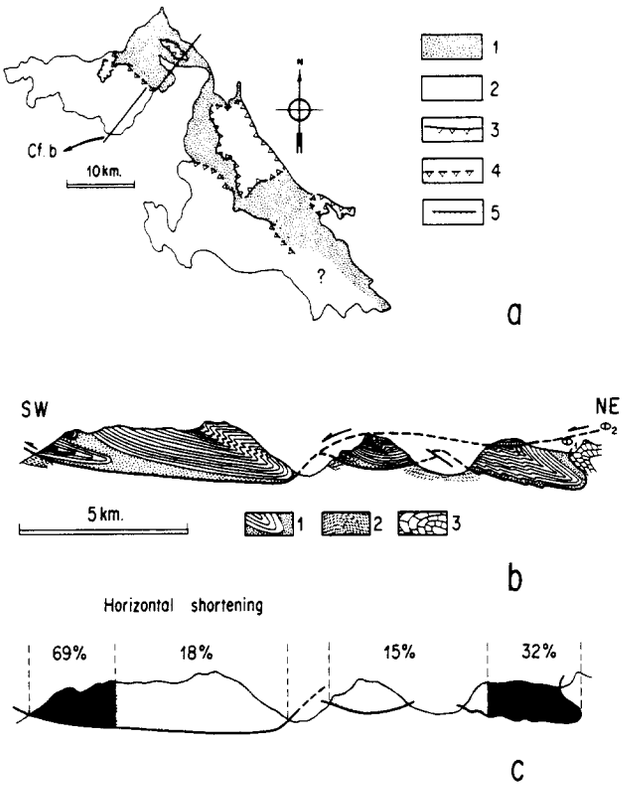

Fig. 3. Structure of the Parpaillon Nappe. (a) Contours of the two units. 1, unit 1; 2, unit 2; 3, observed thrust planes; 4, inferred thrust planes and 5, late thrusts. (b) Geological cross-section; see location in (a). 1, Helminthoid Flysch; 2, sub-Briançonnais Series and 3, Briançonnais Series. (c). Variations of the horizontal shortening along the cross section in (b). From balanced cross sections (Merle 1982).

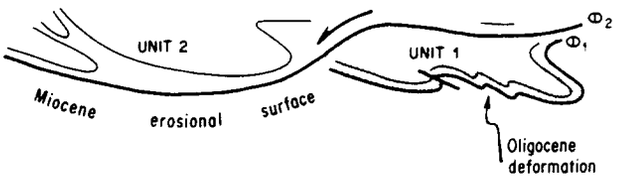

Fig. 4. Sketch illustrating the sliding of unit 2 over unit 1.

around competent clasts and minerals demonstrate a weak extension in the Y direction ($1 < k < 0$).

INCREMENTAL STRAIN

The dominant physical process during $D1$ and $D2$ deformation events was pressure-solution (Durney 1972). Diffusion of quartz and calcite is demonstrated by sharp grain boundaries of quartz and calcite grains associated with seams of residual insoluble minerals (micas) and by fibrous recrystallization of quartz and calcite in numerous veins and pressure-shadows. Estimated temperatures range from 200 to 300°C.

Sequence of veins

Numerous veins filled by calcite fibres were formed during $D1$ and $D2$ deformation. Despite the flattening-type ellipsoid during the $D1$ deformation, vein orienta-

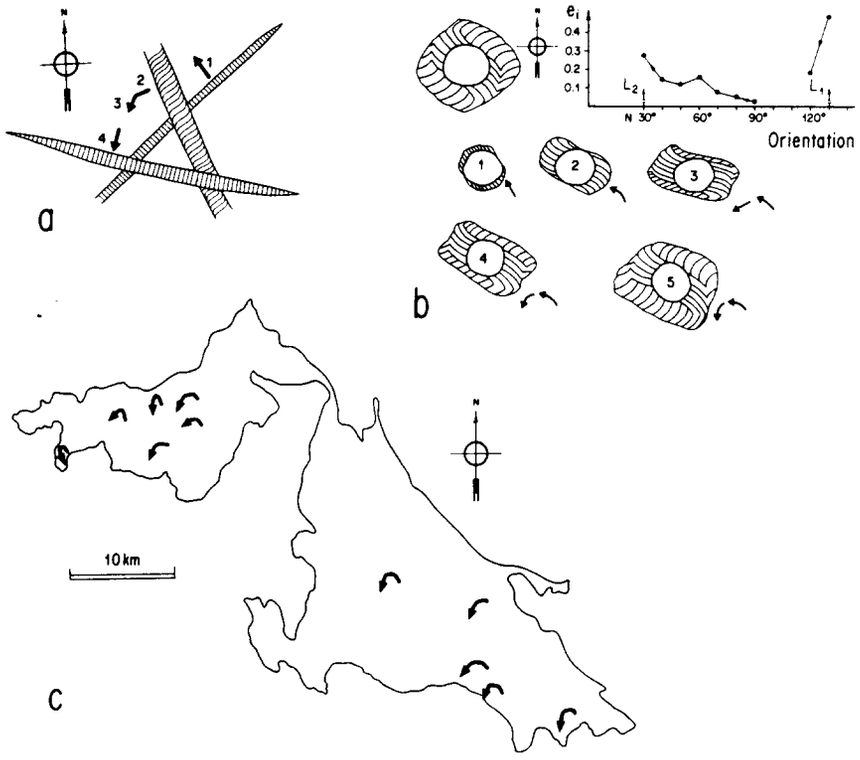

Fig. 5. Incremental strain in unit 2. (a) Progressive sequence of veins indicative of an anticlockwise rotation in the Helminthoid Flysch (SE part of the nappe). (b) Fibrous calcite in pressure shadow zones of spider type around a quartz grain in the basal layers of the Helminthoid Flysch. 1–5 illustrate the progressive evolution of the pressure-shadow. The upper-right diagram shows the variation of incremental extension (e_i) estimated from the fibre lengths as a function of the orientation. The two e_i maxima correspond with the $L1$ and $L2$ stretching lineations. (c) Map of incremental strain data. This Incremental Strain Study has been made in the XY plane.

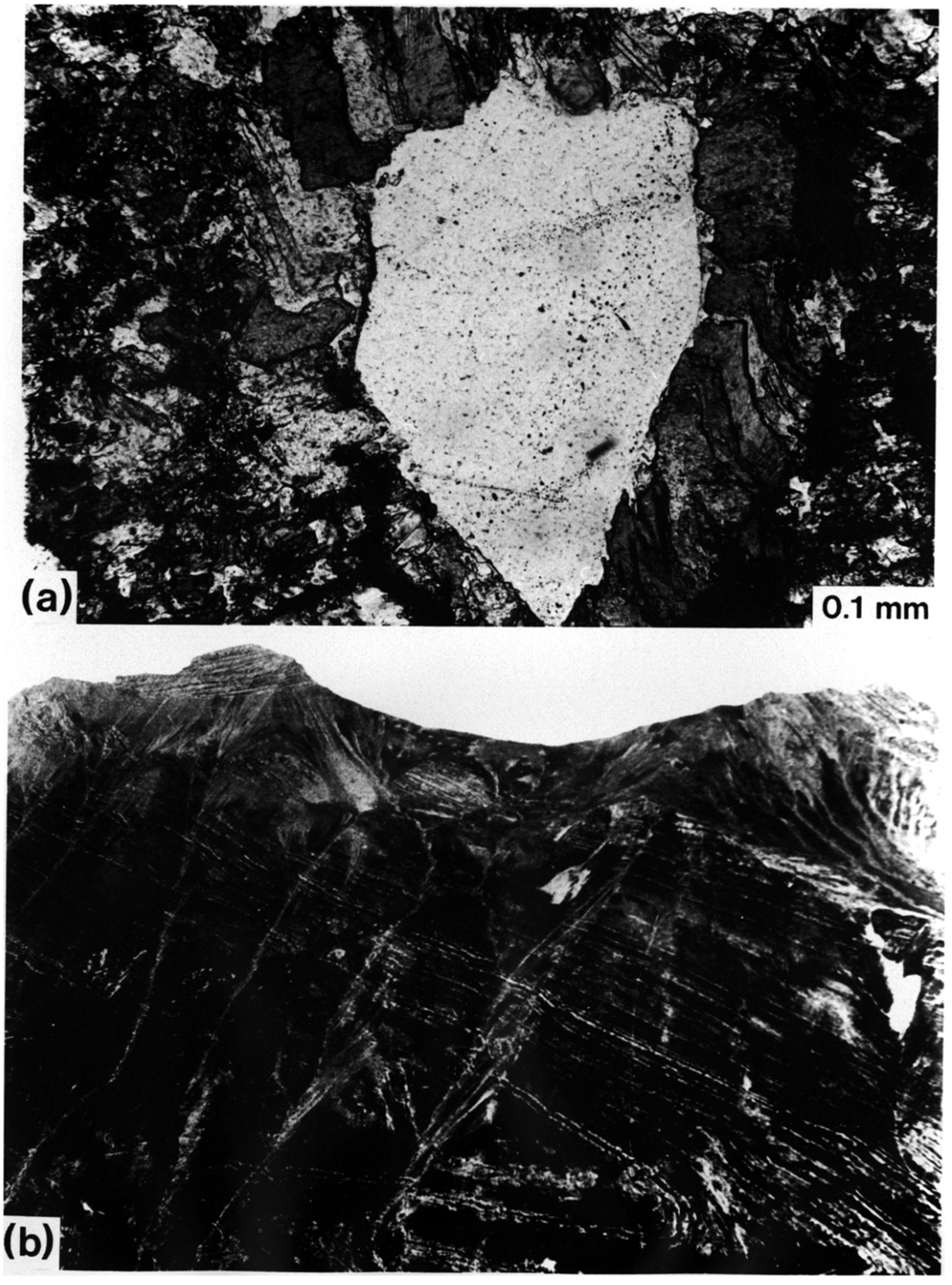

Fig. 6. (a) 'Spider' pressure shadow around a quartz grain. (b) Large-scale $F2$ fold in unit 2. The cliff height is about 1000 m. Layered rocks around the syncline are mostly Helminthoid Flysch. The upper unstratified part of the overturned limb consists of dark shales of the basal layer. Note the tectonic unconformity of the basal sandstone layer in the anticline normal limb at the top left.

tions and cross-cutting relationships in unit 2 are very clear and show a continuous evolution of the stretching history. The first veins to appear imply a stretching direction N140°E, parallel to the $L1$ stretching lineation (Fig. 2a) and the late veins a stretching direction N50°E parallel to the $L2$ stretching direction (Fig. 2b). Intermediate veins show a more or less continuous left-hand rotation (Fig. 5a). When fibres in the veins are sigmoidal, the growth sense of crystal fibres (generally antiaxial, Durney & Ramsay 1973) is in a good agreement with the left-hand rotation.

Pressure shadows

Analysis of pressure shadows at the base of unit 2 allows us to state more precisely the stretching history. At some places where only one cleavage exists, peculiar 'spider' pressure shadows (Figs. 5b and 6a), constituted by calcite fibres around quartz crystals, give an almost complete pattern of the incremental strain evolution. The so-called spider pressure shadows are in fact two superposed pressure shadows where calcite fibres have an antiaxial growth sense. Analysis of incremental stretching was done using the 'pyrite method' (Durney & Ramsay 1973). The diagrams (Fig. 5) show two maxima corresponding with $L1$ and $L2$ stretching lineation directions (Fig. 2), the left-hand rotation displayed with a weaker intensity and a gap (about 30°) between N120°E and N90°E. Rotation and relative magnitude of strain increments have been measured at eleven places in unit 2 (Fig. 5c). Within the limit of the measurement accuracy, it can be concluded that (a) the left hand rotation is represented at the scale of the nappe (unit 2) and is not due to local effects and (b) the apparently distinct $D1$–$D2$ deformation events result from a progressive evolution.

THE EMPLACEMENT

Translation and strain

Arguments have been given which demonstrate a relative continuity between $D1$ and $D2$ incremental strains in unit 2 even if remaining structures are clearly superimposed. The relations between the translation of the nappe and the observed strains can be derived from the progressive character of superposed deformations and the evolution into two units during the $D2$ event. On one hand, we note that unit 1 emplaced on the nummulitic sedimentary cover of the Pelvoux Massif is free of $D2$ deformation in its most external part and strongly refolded with its substratum in the east. On the other hand, $D1$ and $D2$ strain increments are quasi-continuous in unit 2. Therefore, we conclude that the $D2$ deformation in unit 2 is strictly associated with its translation over the unit 1 and emplacement in Embrunais–Ubaye.

Because $F2$ folds axes are orthogonal to the $L2$ stretching lineation, $F2$ major folds are controlled by topographic irregularities of the sole and overturned towards the SW, $L2$ stretching lineations are parallel to the late strain increments, and axes of small-scale $F2$ folds are reoriented into the stretching direction (i.e. sheath folds) at the base of the nappe, we conclude that the $D2$ deformation in unit 2 is characterized by a strong component of horizontal shear associated with a southwestward translation.

For the $D1$ deformation, we find again $F1$ fold axes orthogonal to the NW stretching lineation, small-scale sheath folds at the base of the nappe, major $F1$ folds overturned towards the NW and discrete slips towards the NW along the bedding and the $S1$ cleavage.

Because $D1$ and $D2$ strain increments follow continuously in unit 2 and because a part of the unit 1 is thrust northwestward onto the Pelvoux Massif, we deduce that the $D1$ deformation in the whole nappe results from a northwestward translation.

We argue that strain increments (Fig. 5b) are probably proportional in magnitude and direction to the inferred translations so that the displacement history of the nappe is essentially twofold: firstly toward the NW and secondly toward the SW (Figs. 7 and 8).

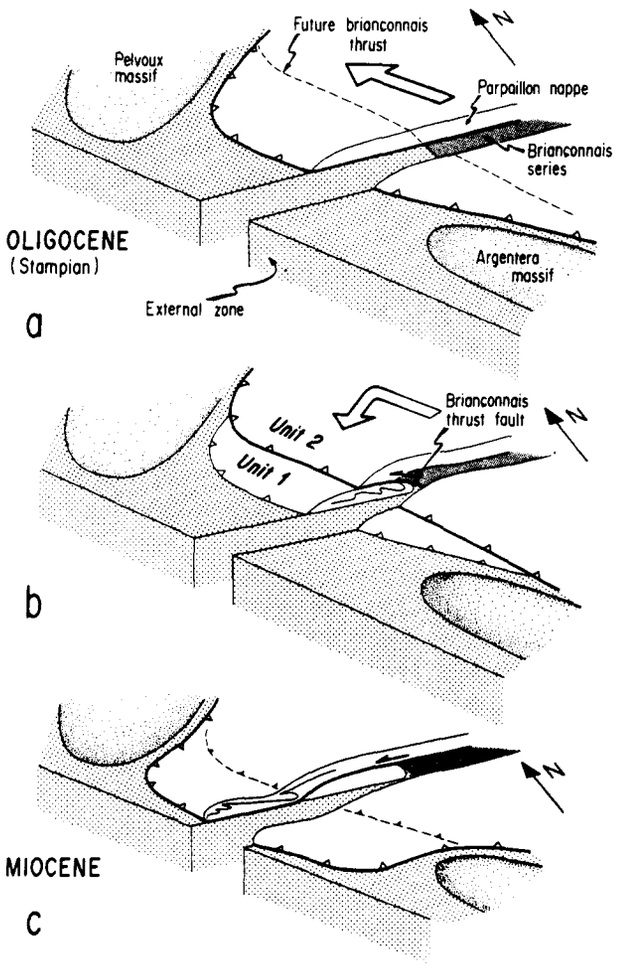

Fig. 7. Cartoon illustrating the kinematic history of the Parpaillon Nappe. (a) Early northwestward translation and emplacement of the whole nappe. (b) Briançonnais thrusting toward the southwest inducing a separation of the nappe in two units. (c) Sliding of unit 2 over unit 1, and late emplacement in Embrunais–Ubaye.

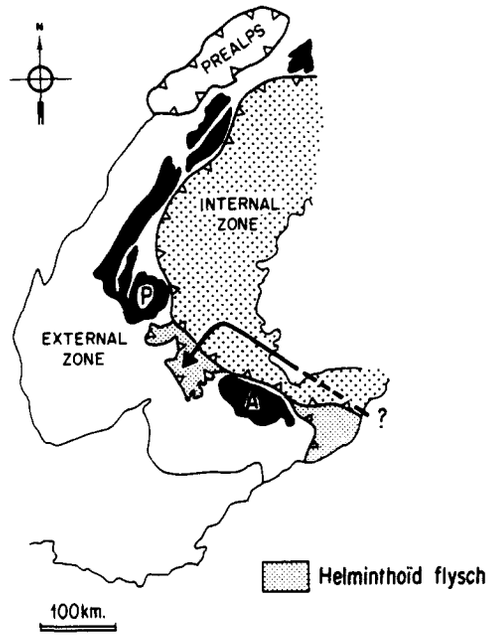

Fig. 8. Location of Ligurian (SE) and Embrunais–Ubaye Helminthoid Flysch in the Western Alps, see Fig. 1. The arrow indicates the inferred translation of the Parpaillon Nappe.

The role of gravity

A first discussion of the role of gravity in the emplacement of the Parpaillon Nappe was given by Kerckhove (1969) and Debelmas & Kerckhove (1973). Their arguments were: (a) that the location of the nappe was in a geologic depression that seems to have acted as a trap for many nappes (Parpaillon, Autapie and sub-Briançonnais nappes) during Tertiary times; (b) the folds of the nappe are truncated at the base and (c) large outcrops of the basal layer at the rear (Fig. 2) can be interpreted as a diverticulation phenomenon. They proposed a gravitational gliding model for the emplacement of the nappe in the Embrunais–Ubaye area. Our structural analysis provides new evidence for this hypothesis.

The increase of the horizontal shortening toward the front of unit 2 (Fig. 3c) is a strong argument in favour of gravity emplacement of this unit in the Embrunais area.

In addition, the large recumbent $F2$ folds are located at the front and in the topographic depressions of the Miocene erosion surface. These folds result from passive folding due to shear-flow perturbations over basal boundary irregularities (Hudleston 1977). Their similar or sub-similar geometry and recumbent attitude is due to high shear strains (Hudleston 1977, Cobbold & Quinquis 1980). Even if they are not specifically related to gravity induced deformations (e.g. Cobbold & Quinquis 1980), their control by the actual topography of the Miocene erosion surface is relevant to the role of gravity.

The $D1$ deformation is characterized everywhere in the nappe by a flat lying cleavage parallel to the stratification and by flattening-type strain ellipsoids resulting from coaxial strain. We deduce a component of gravity spreading (Elliott 1976) in the early deformation and motion. But the total inferred translation from the Ligurean ocean (~200 km) cannot be achieved by spreading alone. Nevertheless, we believe that a component of rigid body gliding must be taken into account for the northwestward emplacement because the very large surface (3600 km^2) and very thin thickness (actually 1000 m) of the nappe cannot mechanically allow an emplacement by a push from the rear.

The Parpaillon Nappe in the Western Alps

The inferred translation of the Parpaillon Nappe indicates a northward motion during the Eocene. This interpretation is consistent with palaeogeographical studies (Haccard *et al.* 1972, Kerckhove 1980) that locate the sedimentation area of the Helminthoid Flysch in the Ligurean ocean. Moreover, this could be correlated with the early N–S compression during the Eocene (Lemoine 1972, Caby 1973, Gratier *et al.* 1973, Vialon 1974, Subieta 1977, Siddans 1979, Gourlay 1982), well known in the external domain of French Alps. Our study seems to indicate, as suggested before by Caby (1973), that a N–S shortening occurred at the same time in the most superficial formations of the internal domain (Fig. 8). An alternative hypothesis to obtain large northwards translation is to make sinistral strike slip displacement along N–S faults (Ricou 1980, Ricou & Siddans in press). But, for the Parpaillon Nappe, the close relation between strain and displacement seems to indicate a tangential translation during N–S compression, although this is not inconsistent with major sinistral strike slip at the same time.

We conclude that the Helminthoid Flysch nappes are superficial and gravity driven. Nevertheless, we suggest that the strong variation in the translation first northwestward and second southwestward may have a deep significance in the kinematics of the Alpine collision.

CONCLUSIONS

Our main conclusions are the following.

(1) The Parpaillon Nappe is a clear example of a superposed structure resulting from a progressive deformation.

(2) The two deformation events are associated with a twofold translation; firstly NW and secondly SW.

(3) The finite strain pattern and the incremental strain history favour a gravity interpretation for nappe emplacement.

(4) The tectonic history of the Parpaillon Nappe provides a new argument for a generalized N–S compression in the Western Alps during the Eocene followed by a E–W compression during the late Oligocene and the Miocene.

Acknowledgements—We are indebted to our colleagues of the 'Laboratoire de Géologie Structurale' of the Rennes University (CNRS LP N° 04661) principally Pierre Choukroune, Peter Cobbold,

Denis Gapais and Lyal Harris. Their comments and suggestions have been very useful at different steps of the work. Thanks are also due to Sue Treagus and the two anonymous referees.

REFERENCES

Berthé, D., Choukroune, P. & Jegouzo, P. 1979. Orthogneiss, mylonite and non coaxial deformation of granites: the example of the South Armorican shear zone. *J. Struct. Geol.* **1**, 31–42.

Brun, J. P. & Merle, O. 1982. La Nappe du Parpaillon (Flysch à Helminthoïdes de l'Embrumais–Ubaye): II. Mécanismes de mise en place. 9e *Réun. Ann. Sci. Terre*, Jussieu (Paris), 98.

Caby, R. 1973. Les Plis transversaux dans les Alpes Occidentales: implication pour la genèse de la chaîne alpine. *Bull. Soc. géol. Fr.*, 7 *Ser.* **15**, 624–634.

Choukroune, P. 1971. Contribution à l'étude des mécanismes de la déformation avec schistosité grâce aux cristallisations syncinématiques dans les 'zones abritées' ('pressure shadows'). *Bull. Soc. géol. Fr.*, 7 *Ser.* **13**, 3–4, 257–271.

Choukroune, P. & Lagarde, J. L. 1977. Plan de schistosité et déformation rotationnelle: l'exemple du gneiss de Champtoceaux. *C. r. hebd. Séanc. Acad. Sci., Paris* **284**, 2331–2334.

Cobbold, P. R. & Quinquis, H. 1980. Development of sheath folds in shear regimes. *J. Struct. Geol.* **2**, 119–126.

Debelmas, J. & Kerckhove, C. 1973. Large gravity nappes in the French–Italian and French–Swiss Alps. In: *Gravity and Tectonics* (edited by De Jong, K. & Scholten, R.). Wiley, New York, 189–200.

Durney, D. W. 1972. Solution transfer, an important geological deformation mechanism. *Nature, Lond.* **235**, 315–317.

Durney, D. W. & Ramsay, J. G. 1973. Incremental strains measured by syntectonic crystal growths. In: *Gravity and Tectonics* (edited by De Jong, K. & Scholten, R.). Wiley, New York, 67–96.

Elliott, D. 1976. The motion of thrust sheets. *J. geophys. Res.* **81**, 949–963.

Elliott, D. 1977. Some aspects of the geometry and mechanics of thrust belts. Part I. 8th Annual Seminar Can. Soc. Petrol. Geol., University of Calgary.

Gourlay, P. 1982. La déformation dans le couloir du Bonnant entre Mont-Blanc et Belledonne (Alpes françaises). *C. r. hebd. Séanc. Acad. Sci., Paris* **294**, 1291–1294.

Gratier, J. P., Lejeune, B. & Vergne, J. L. 1973. Etude des déformations de la couverture et des bordures sédimentaires des massifs cristallins externes de Belledonne, Grandes Rousses et Pelvoux. Thèse 3e cycle, Grenoble.

Haccard, D., Lorenz, C. & Grandjacquet, C. 1972. Essai sur l'évolution tectogénétique de la liaison Alpes–Apennins. *Mém. Soc. géol. Fr.* **11**, 309–341.

Hossack, J. R. 1979. The use of balanced cross sections in the calculation of orogenic contraction: a review. *J. geol. Soc. Lond.* **136**, 705–711.

Hudleston, P. J. 1977. Similar folds, recumbent folds and gravity tectonics in ice and rocks. *J. Geol.* **85**, 113–122.

Kerckhove, C. 1969. La zone du flysch dans les nappes de l'Embrunais–Ubaye. *Géol. Alpine* **45**, 5–204.

Kerckhove, C. 1980. Panorama des séries synorogéniques des Alpes Occidentales. In: *Evolutions Géologiques de la France* (edited by Autran, A. & Dercourt, J.). 26e Congrès Géol. Intern., colloque C7, *Mém. Bur. Rech. geol. min. Fr.* **107**, 241.

Lagarde, J. L. 1978. La déformation des roches dans les zones à schistosité sub-horizontale. Thèse 3e cycle, Rennes.

Latreille, M. 1961. Les nappes de l'Embrunais entre Durande et Haut-Drac. Thèse, Grenoble, 1958. *Mém. Serv. Carte géol. dét. Fr.*

Lemoine, M. 1972. Rythme et modalités des plissements superposés dans les chaînes sub-alpines méridionales des Alpes Occidentales Françaises. *Geol. Rdsch.* **61**, 975–1010.

Maury, P. & Ricou, L. E. 1983. Le décrochement subbriançonnais: une nouvelle interprétation de la limite interne-externe des Alpes franco-italiennes. *Revue Géogr. phys. Géol. dyn.* **24**, 3–22.

Merle, O. 1982a. Mise en place séquentielle de la Nappe de Parpaillon (Flysch à Helminthoïdes, Alpes Occidentales). *C. r. hebd. Séanc. Acad. Sci., Paris* **294**, 603–606.

Merle, O. 1982b. Cinématique et déformation de la Nappe du Parpaillon (Flysch à Helminthoïdes de l'Embrunais–Ubaye, Alpes Occidentales). Thèse 3e cycle, Rennes.

Merle, O. & Brun, J. P. 1981. La déformation polyphasée de la Nappe du Parpaillon (Flysch à Helminthoïdes): un résultat de la déformation progressive associée à une translation non rectiligne. *C. r. hebd. Séanc. Acad. Sci., Paris* **292**, 343–346.

Ramsay, J. G. 1967. *Folding and Fracturing of Rocks*. McGraw-Hill, New York.

Ricou, L. E. 1980. La zone sub-Briançonnaise des Alpes occidentales interprétée comme la trace d'un ample décrochement senestre sub-méridien. *C. r. hebd. Séanc. Acad. Sci., Paris* **290**, 835–838.

Ricou, L. E. & Siddans, A. W. B. in press. Collision tectonics in Western Alps. *Spec. Publs geol. Soc. Lond.*

Rutter, E. H. 1976. The kinetics of rocks deformation by pressure solution. *Phil. Trans. R. Soc. Lond.* **A283**, 203–219.

Siddans, A. W. B. 1979. Arcuate fold and thrust patterns in the subalpine chains of southeast France. *J. Struct. Geol.* **1**, 117–126.

Subieta, T. A. 1977. Analyse quantitative de la déformation dans un secteur de la zone externe des Alpes. Thèse 3e cycle, Montpellier.

Tricart, P. 1980. Tectoniques superposées dans les Alpes Occidentales au Sud du Pelvoux. Evolution structurale d'une chaîne de collision. Thèse, Strasbourg.

Vialon, P. 1974. Les déformations 'synschisteuses' superposées en Dauphiné. Leur place dans la collision des éléments du socle pré-alpin; conséquences pétrostructurales. *Bull. Suisse Minéral. Pétrogr.* **54**, 663–690.